

Finite Element Simulations of the Contact Stress between Rotary Sinus Lift Kit and Sinus Membrane during Lifting Process

Ching-Chieh Huang¹, Li-Wen Chen², Dong-Feng Wu², Yung-Chuan Chen^{2*}

¹Metal Industries Research & Development Centre

²Department of Vehicle Engineering, National Pingtung University of Science and Technology

E-mail: chuan@mail.npust.edu.tw

Abstract: In this study, a three-dimensional elastic-plastic finite element model is used to simulate the lifting process of the sinus membrane using a rotary sinus lift kit. The effects of the edge radius of sinus lift kit and the feeding rate on the contact stress of sinus membrane are explored. Three different edge radii, i.e. 0.4, 0.6 and 1.0 mm, and three different feeding rates, 1, 3 and 5 mm/s, are discussed. The results show that a rotary sinus lift kit with a smaller edge radius has a lower contact stress distribution on the sinus membrane. The results also indicate that a higher feeding rate results in a larger plastic zone on the sinus membrane.

[Ching-Chieh Huang, Li-Wen Chen, Dong-Feng Wu, Yung-Chuan Chen. **Finite Element Simulations of the Contact Stress between Rotary Sinus Lift Kit and Sinus Membrane during Lifting Process.** Life Science Journal. 2012; 9(2):167-171] (ISSN:1097-8135). <http://www.lifesciencesite.com>. 28

Keywords: Sinus Lifting, Contact Stress, Feeding Rate, Finite Element Analysis

1. Introduction

When the height of alveolar bone is not enough, the sinus lift approach must be applied to add the bone height such that the success rate of dental implantation can be enhanced. To do this, in the past few years, the rotary sinus lift approach was developed to substitute the traditional osteotome technique. Sinus lift surgery can be done safely and accurately by using the rotary sinus lift approach. Two maxillary sinuses are respectively placed on upper sides of roots of molars in the form of cavities surrounded by bones. When a molar on maxilla is extracted, the insufficient bone mass of maxilla gives a difficulty for the placement of dental implants. The method of maxillary sinus lifting procedure for the placement of dental implants was firstly introduced by Tatum [1] in 1976. The procedure was intended to increase the height of alveolar bone in posterior maxilla. Traditionally, when the remaining height is less than 5mm, open window technique should be taken since longer time is required for the treatment. However, if the remaining height is no less than 5mm, the osteotome technique is used to increase the height of alveolar bone [2~5]. The investigation by Fugazzatto and Vlassis [6] indicated that no differences were observed in implant survival rates as the osteotome or the open window technique was used. Due to less surgery trauma and less postoperative reaction, the osteotome technique has been used clinically in recent years [7]. The experimental study of John and Steen [8] indicated that the damage of the maxillary sinus membrane was the main complication of maxillary sinus lifting. Vernamonte et al. [9] showed that shaking during knocking process may lead to complications of brain

or ear cavity damages and make the patient feel uncomfortable. At present, the rotary sinus lift approach has been developed to replace the traditional knocking approach so that sinus lifting can be carried out in a safer and more precise way [10~15]. Huang et al. [16] and Tu et al. [17] used a three-dimensional finite element model to simulate the bone temperature rise during drilling process.

This research aims to investigate the effects of the edge radius design of rotary sinus lift kit on the contact stress of the sinus membrane during sinus lifting. The contact stress distributions on the sinus membrane for various feeding rates are also explored. Accordingly, in this study, a three-dimensional finite element model is proposed to simulate the contact behavior between the sinus membrane and the sinus lift kit. The results can provide a reference for the design of rotary sinus lift kit.

2. Finite Element Model

The rotary lifting process of sinus membrane is explored in this study. The effect of feeding rate on the deformation of sinus membrane during rotary lifting process is also studied. A three-dimensional elastic-plastic finite element model is used to simulate the contact behavior between the sinus membrane and the sinus lift kit during the lifting process. Because the shape of sinus membrane is changed over time during the lifting process, dynamic simulations are performed using the commercial ABAQUS/Explicit package. It is known that shape of sinus membrane is complicated. For simplicity, the sinus membrane is modeled as a thin disk with a diameter of 40 mm and a thickness of 0.5 mm [18]. The simplified model is established

according to the maximum width in a single tooth loss area in alveolar bone and the size of the standard of human alveolar bone. In this study, a CAS rotary sinus lift kit (Korea) is employed. The model of the CAS sinus lift kit is constructed by using the software Solidworks, as shown in Fig. 1. The CAS CAD model is later input to ABAQUS/CAE and assembled with sinus membrane model. In performing the simulations, the contact behavior between the sinus membrane and the sinus lift kit is modeled using surface to surface contact discretisation.

Figure 2 shows the configuration of the contact model. Finite element models of the sinus membrane and the sinus lift kit are shown in Fig. 3. The nodes on the circumference surface of the sinus membrane are fixed during the lifting process. In this model, the element types selected for the sinus membrane and the sinus lift kit are 8-node brick elements C3D8 and 4-node tetrahedron elements C3D4, respectively. The friction coefficient between lift kit and sinus membrane is set as 0.3. There are 6005 nodes and 4736 elements in sinus membrane, 1056 nodes and 4450 elements in sinus lift kit. The mechanical properties of the sinus membrane used in finite element simulations are listed in Table 1 [18~19]. The material of the lift kit is stainless steel SUS420, the same as those used in normal drills for oral implant [20].

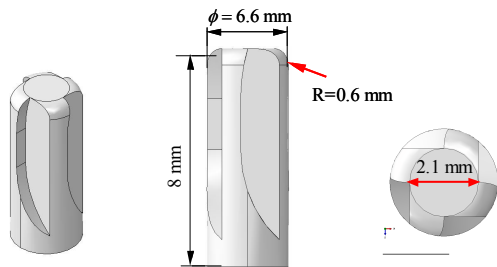


Fig. 1 Appearance of the CAS rotary sinus lift kit.

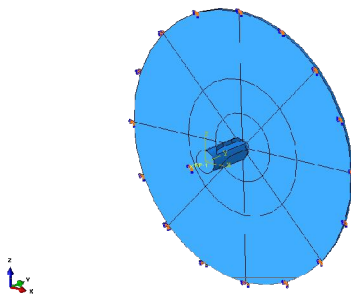


Fig. 2 The configuration of the contact model.

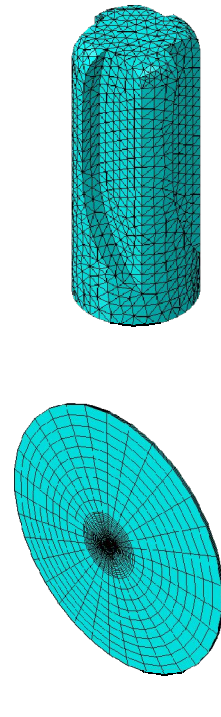


Fig. 3 The finite element models of sinus membrane and sinus lift kit

Table 1. Mechanical properties of sinus membrane and lift kit used in finite element model [18-20].

Properties of materials	sinus lift kit	Sinus membrane
Density (Kg/m ³)	7840	1000
Young's modulus(MPa)	210000	70.3
Yielding strength (MPa)	585	3.91
Tensile strength (MPa)	760	8.6
Poisson's ratio	0.24	0.45

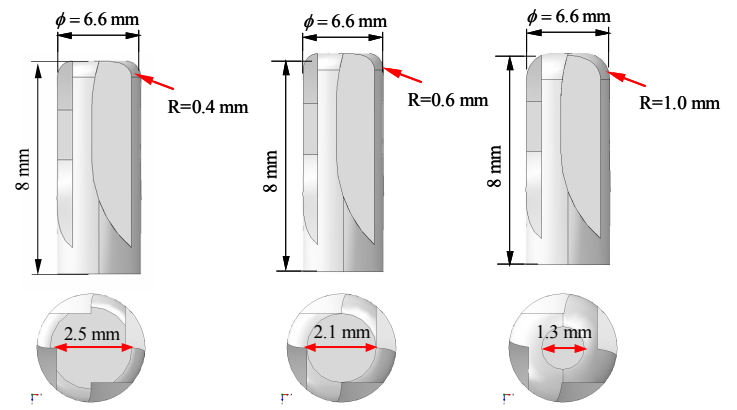


Fig. 4 Appearances of sinus lift kit with different edge radius designs

3. Results and Discussion

As shown in Fig. 1, the edge radius R of the original KIT lift kit is 0.6 mm. In this study, the edge radius is changed and its effect on the contact stress is explored. Three different radii R and three different feeding rates are investigated.

3.1 Lift kit with different radius designs

The sinus lift kits with different radii R , i.e. 0.4, 0.6 and 1.0 mm, are shown in Fig. 4. The rotation speed of each lift kit is fixed as 800 rpm in simulations and the total lifting time is 1 second. Figure 5 shows the von-Mises stress distributions on the sinus membrane for sinus lift kit with different radius designs at lifting displacement 1 mm. The maximum von-Mises occurs on the membrane are 0.58, 0.6 and 0.75 MPa for the lift kit with radius of $R=0.4$, 0.6 and 1.0 mm, respectively. The results indicate that the maximum von-Mises increases with increasing corner radius. This can be attributed to the variation of contact area between the sinus membrane and the lift kit. It can be seen from Fig. 4 the contact area decreases as the edge radius increases. A smaller contact area results in a larger contact stress. All the maximum von-Mises stresses stated above are less than the yield strength 3.91 MPa of the sinus membrane. It means that the sinus membrane can sustain 1 mm lifting displacement for the lift approach with all the three different radius designs and no structure damage will occur.

The contact von-Mises stress distributions on the sinus membrane for a lifting displacement of 3 mm is shown in Fig. 6. The maximum von-Mises occurs on the membrane are 2.9, 3.25 and 4.2 MPa for the lift kit with a radius of $R=0.4$, 0.6 and 1.0 mm, respectively. Compared with Fig. 5, it can be observed that contact stresses increase obviously as the lifting displacement increases from 1 mm to 3 mm. In the case of lifting displacement 3 mm, the membrane stress caused by the lift kit with a radius of $R=1.0$ mm exceeds the yielding strength of the sinus membrane. Figure 7 presents the contact von-Mises stress distribution on the sinus membrane for a lifting displacement of 5 mm. In Fig. 7, the maximum von-Mises occurs on the membrane are 3.4, 4.3 and 4.9 MPa for the lift kit with radius of $R=0.4$, 0.6 and 1.0 mm, respectively. With this lifting displacement, all the maximum stress exceeds the yield strength of sinus membrane but is still less than its tensile strength. It should be noted that a stress larger than the yield stress will result in plastic deformation in sinus membrane even though the load is released after surgery. From the results shown above, it can be concluded that the sinus lift approach with a smaller edge radius, in this study $R=0.4$ mm, has a lower contact stress distribution on the sinus

membrane than those with other radius designs.

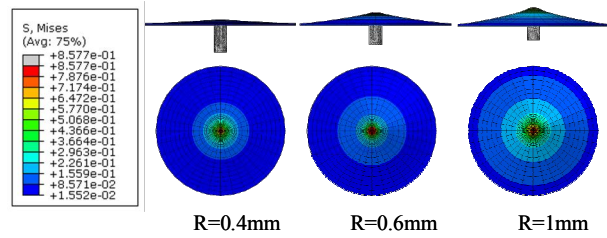


Fig. 5 The von-Mises stress distributions on the sinus membrane for lifting displacement 1 mm

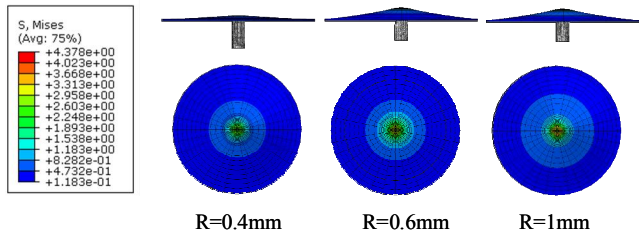


Fig. 6 The von-Mises stress distributions on the sinus membrane for lifting displacement 3 mm

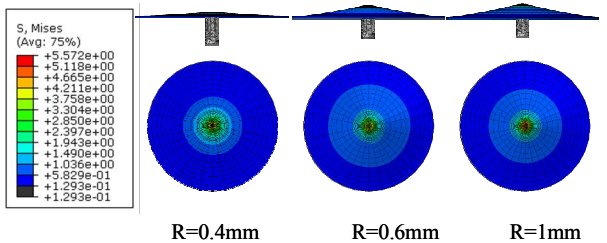


Fig. 7 The von-Mises stress distributions on the sinus membrane for lifting displacement 5 mm

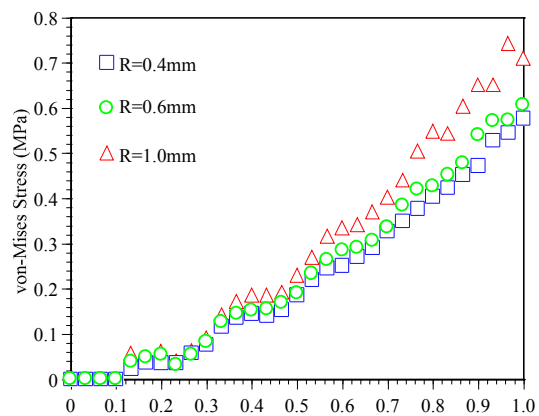


Fig. 8 Variations in von-Mises stress with lifting time at lifting displacement 1 mm for various corner radii

Figures 8~10 plot the variations of the von-Mises stress with the lifting time for different corner radii and lifting displacements. In these figures, the stresses are taken at the center point of the sinus membrane. The results of Figs. 8~10 confirm that the von-Mises stress accumulated in the membrane increases as the lifting time increases.

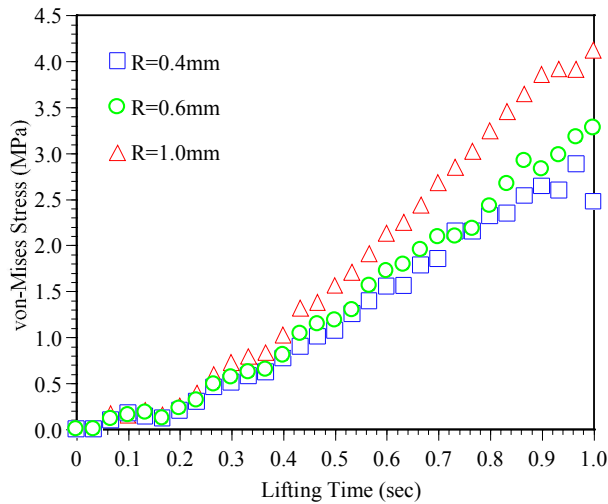


Fig. 9 Variations in von-Mises stress with lifting time at lifting displacement 3 mm for various corner radii

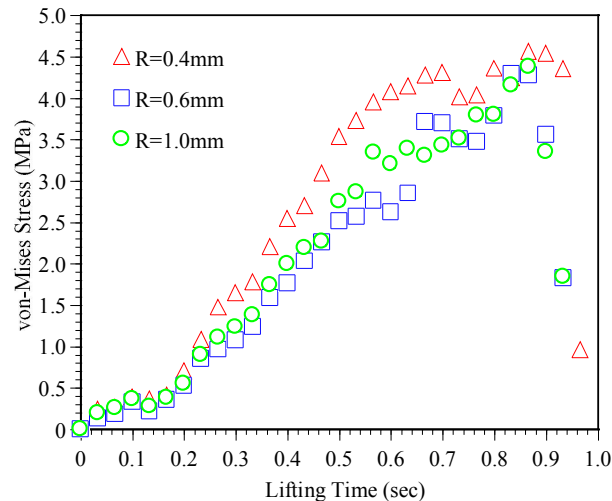


Fig. 10 Variations in von-Mises stress with lifting time at lifting displacement 5 mm for various corner radii

3.2 Lift approach with different feeding rate

In the following discussions, a sinus lift kit with an edge radius of R=0.6 mm is used. The rotation speed of the lift kit is fixed as 800 rpm in simulations and the total lifting time is 1 second. The forces applied to the sinus membrane are explored during the lifting process. Figure 11 shows the variation in applied force with lifting time for various feeding

rates. Three different feeding rates, i.e. 1, 3, 5 mm/s, are discussed. From the simulation results, it can be observed that the feeding rate has a significant influence on the applied force. A larger feeding rate results in a larger applied force on the sinus membrane. This can induce a larger contact stress on the sinus membrane. Figure 12 presents the von-Mises stress distributions on the sinus membrane for various feeding rates. In order to understand the effect of feeding rate on the plastic deformation region in sinus membrane, the stress exceeds yielding strength 3.91 MPa is presented in gray color, as shown in Fig. 12. It is easy to see that the plastic zone size increases with increasing feeding rate. The plastic zone size can be obtained as 0, 0 and 3.04 mm for feeding rate of 1, 3 and 5 mm/s, respectively.

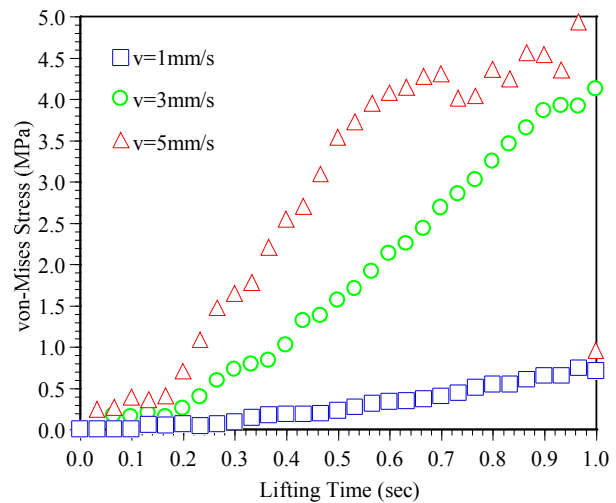


Fig. 11 Variation in applied force with lifting time as function of feeding rate

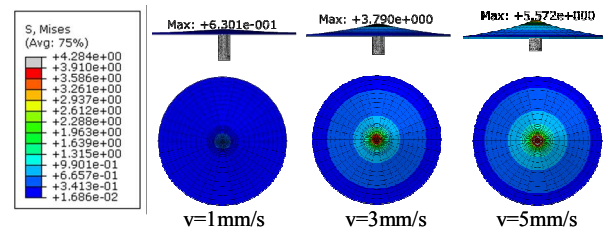


Fig. 12 The von-Mises stress distributions on the sinus membrane for various feeding rate

4. Conclusion

This study proposes a three-dimensional elastic-plastic finite element model to simulate the contact behavior between the KIT rotary sinus lift kit and the sinus membrane during lifting process. The effects of the edge radius of the sinus lift kit and the feeding rate on the contact stress of sinus membrane are explored. Based on the numerical results, the following conclusions can be drawn:

1. A rotary sinus lift kit with a smaller edge radius design can has a lower contact stress distribution on the sinus membrane.
2. A higher feeding rate results in a larger plastic zone on the sinus membrane.
3. This result can provide a reference for manufacturers or relevant organizations in developing more advanced rotary lift kits.

Corresponding Author:

Yung-Chuan Chen

E-mail : chuan@mail.npust.edu.tw

References

1. Tatum OH. Maxillary and sinus implant reconstruction. *Dent Clin North Am*, 1986, 30: 207–229.
2. Davarpanah M, Martinez H, Tecucianu JF, Hage G, Lazzara R. The friction free osteotome technique: introduction of a modified approach. *Int J Periodontics Restor Dent*, 2001, 21: 599–607.
3. Summers RB. The osteotome technique: Part 3—Less invasive methods of elevating the sinus floor. *Compend Contin Educ Dent*, 1994, 15: 698–710.
4. Bruschi GB, Scipioni A, Calesini G, Bruschi E. Localized management of sinus floor with simultaneous implant placement: a clinical report. *Int J Oral Maxillofac Implants*, 1998, 13: 219–226.
5. Cavicchia F, Bravi F, Petrelli G. Localized augmentation of the maxillary sinus floor through a coronal approach for the placement of implants. *Int J Periodontics Restor Dent*, 2001, 21: 475–485.
6. Fugazzatto PA, Vlassis J. Long-term success of sinus augmentation using various surgical approaches and grafting materials. *Int J Oral Maxillofac Implants*, 1998, 13: 52–58.
7. Attard NJ, Zarb GA. Long-term treatment outcomes in edentulous patients with implant-fixed prostheses: the Toronto study. *Int J Prosthodont*, 2004, 17: 417–424.
8. John J, Steen SP, Anthony JO. Varying treatment strategies for reconstruction of maxillary atrophy with implants: results in 98 patients. *Int J Oral Maxillofac Surg*, 1994, 52: 21–216.
9. Vernamonte S, Mauro V, Vernamonte S. An unusual complication of osteotome sinus floor elevation: benign paroxysmal positional vertigo. *Int J Oral Maxillofac Surg*, 2011, 40: 216–218.
10. <http://www.sinustech.co.kr>
11. <http://www.denti-mate.com>
12. <http://www.dioimplant.com>
13. <http://en.osstem.com>
14. <http://www.dentium.com>
15. <http://www.megagen.com>
16. Huang CC, Liu YC, Chen LW, Chen YC. Temperature rise of alveolar bone during dental implant drilling using the finite element simulation. *Life Sci J*, 2010, 7 (1): 68–72.
17. Tu YK, Hong YY, Chen YC. Finite element modeling of kirschner pin and bone thermal contact during drilling. *Life Sci J*, 2009, 6 (4): 23–27.
18. Pommer B, Unger E, Suto D, Hack N, Watzek G. Mechanical properties of the Schneiderian membrane in vitro. *Clin Oral Impl Res*, 2009, 20: 633–637.
19. Hu Q, Xu Q, Yao Y, et al. Computer aided analysis in maxillary sinus surgery. *APCMBE, IFMBE Proceedings*, 2008, 19: 737–740.
20. <http://www.matweb.com>

Received December 2, 2011